Mechanical Anisotropies of Shales

Rune M Holt, NTNU & SINTEF

With contributions from Andreas Bauer & Erling Fjær (SINTEF & NTNU), Per Horsrud (Statoil), Olav-Magnar Nes (Det Norske Oljeselskap) & Jørn F Stenebråten (SINTEF)

SINTEF NTNU

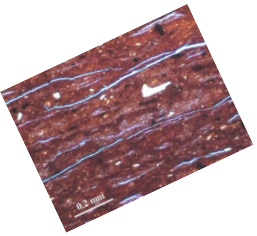

Shales are anisotropic…

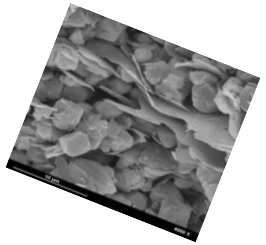

- **Seismic Anisotropy**
  - Influence on AVO, Travel times, Shear Wave Splitting
  - Thomsen-parameters ε, γ and δ
- **Rock Mechanical Anisotropy**
  - We are aware…
  - .. but do we care… ?

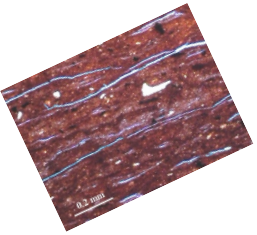

Shales are anisotropic…

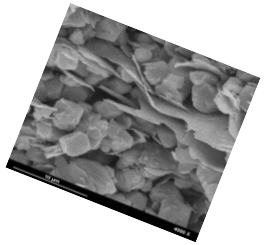

- **Dynamic Anisotropy**
  - Wave velocity anisotropy can be measured quickly in the lab
  - In principle, only one core needed
- **Static Anisotropy**
  - Time consuming tests
  - Several cores needed
- Static ≠ Dynamic moduli;
  What about their anisotropies?

Dynamic moduli

- We determine directly 4 elastic coefficients from ultrasonic measurements (+ Thomsen's ε and γ):

$$C_{11} = \rho v_{Pr}^2, \quad C_{33} = \rho v_{Pz}^2 \qquad \varepsilon = \frac{C_{11} - C_{33}}{2C_{33}}$$

$$C_{44} = \rho v_{Sz}^2, \quad C_{66} = \rho v_{Sr}^2 \qquad \gamma = \frac{C_{66} - C_{44}}{2C_{44}}$$

- From the angular dependence of v_P we find C_{13} (=>Thomsen's δ):

$$\delta = \frac{(C_{13} + C_{44})^2 - (C_{33} - C_{44})^2}{2C_{33}(C_{33} - C_{44})}$$

$$C_{13} = (C_{33} - C_{44})\sqrt{1 + \frac{2C_{33}\delta}{C_{33} - C_{44}}} - C_{44}$$

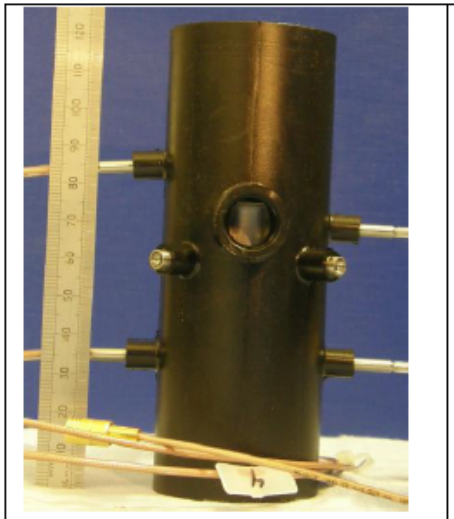

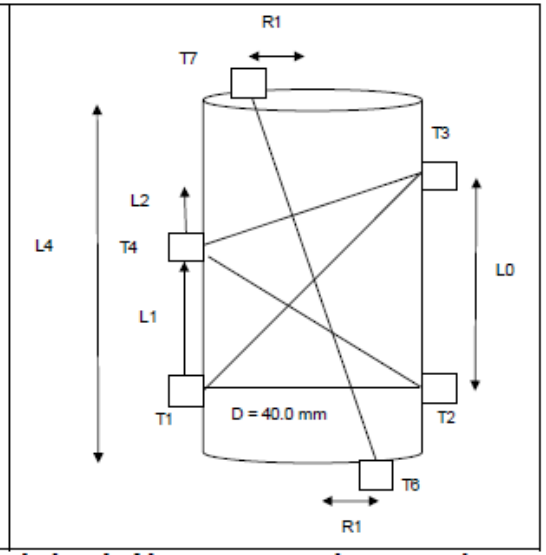

Static Moduli

- Static moduli: Slopes of stress vs. strain curves
- Different moduli require different stress paths, e.g.
  - Uniaxial strain ⊥ symmetry plane (|| symmetry (z-)) axis:

$$\left(\frac{\Delta\sigma_z}{\Delta\varepsilon_z}\right)_{\varepsilon_r=0} = C_{33} \qquad \left(\frac{\Delta\sigma_r}{\Delta\varepsilon_z}\right)_{\varepsilon_r=0} = C_{13}$$

  - Uniaxial stress ("triaxial") tests:
    - Load || symmetry (z-) axis

$$\left(\frac{\Delta\sigma_z}{\Delta\varepsilon_z}\right)_{\Delta\sigma_r=0} = E_{\perp} = \frac{\left[C_{33}(C_{11}-C_{66})-C_{13}^2\right]}{(C_{11}-C_{66})}$$

    - Load ⊥ symmetry (z-) axis

$$\left(\frac{\Delta\sigma_z}{\Delta\varepsilon_z}\right)_{\Delta\sigma_r=0} = E_{\mathrm{P}} = \frac{4C_{66}[C_{33}(C_{11}-C_{66})-C_{13}^2]}{(C_{11}C_{33}-C_{13}^2)}$$

  - Constant mean stress (z is symmetry axis):

$$\left(\frac{\Delta\sigma_z}{\Delta\varepsilon_z}\right)_{\Delta\bar{\sigma}=0} = f(C_{11},C_{33},C_{66},C_{13}) \rightarrow 2C_{44}$$ (weak anisotropy)

Bounds on Transversely Isotropic elastic moduli

- Positive definiteness of elastic energy $\rightarrow$

$$C_{44} \,\&\, C_{66} > 0$$

$$E_{\perp} \,\&\, E_{\mathrm{P}} > 0 \Rightarrow C_{11} > C_{66}$$

$$(C_{11} - C_{66})C_{33} - C_{13}^2 > 0$$

$$\Leftrightarrow -\sqrt{(C_{11} - C_{66})C_{33}} < C_{13} < \sqrt{(C_{11} - C_{66})C_{33}}$$

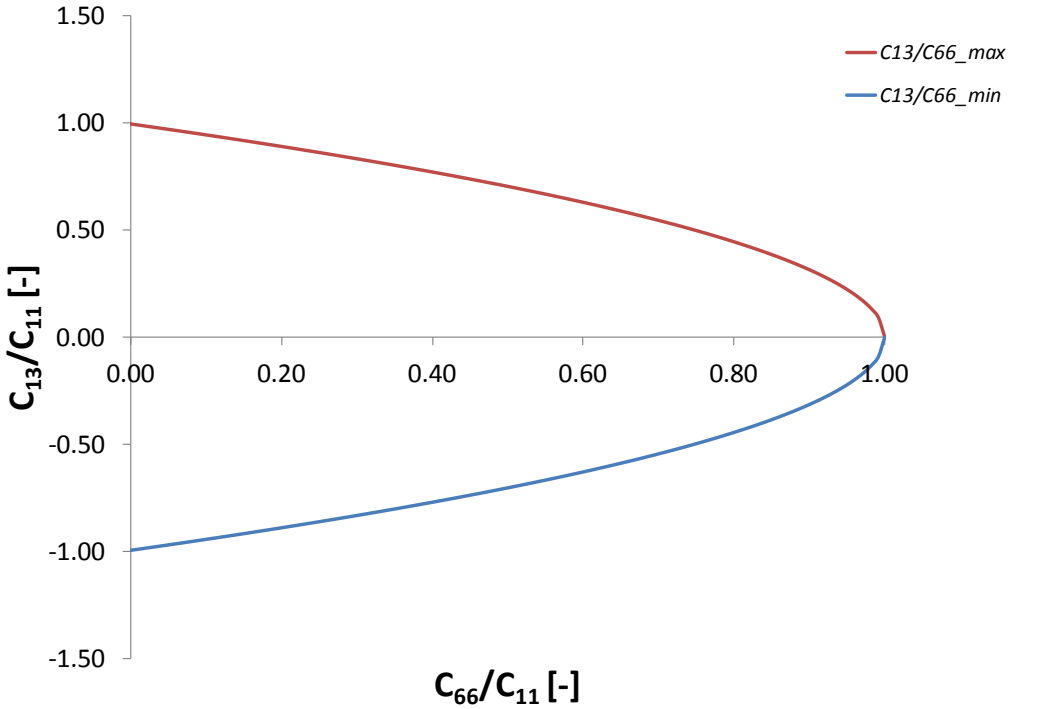

Bounds on Thomsen's δ

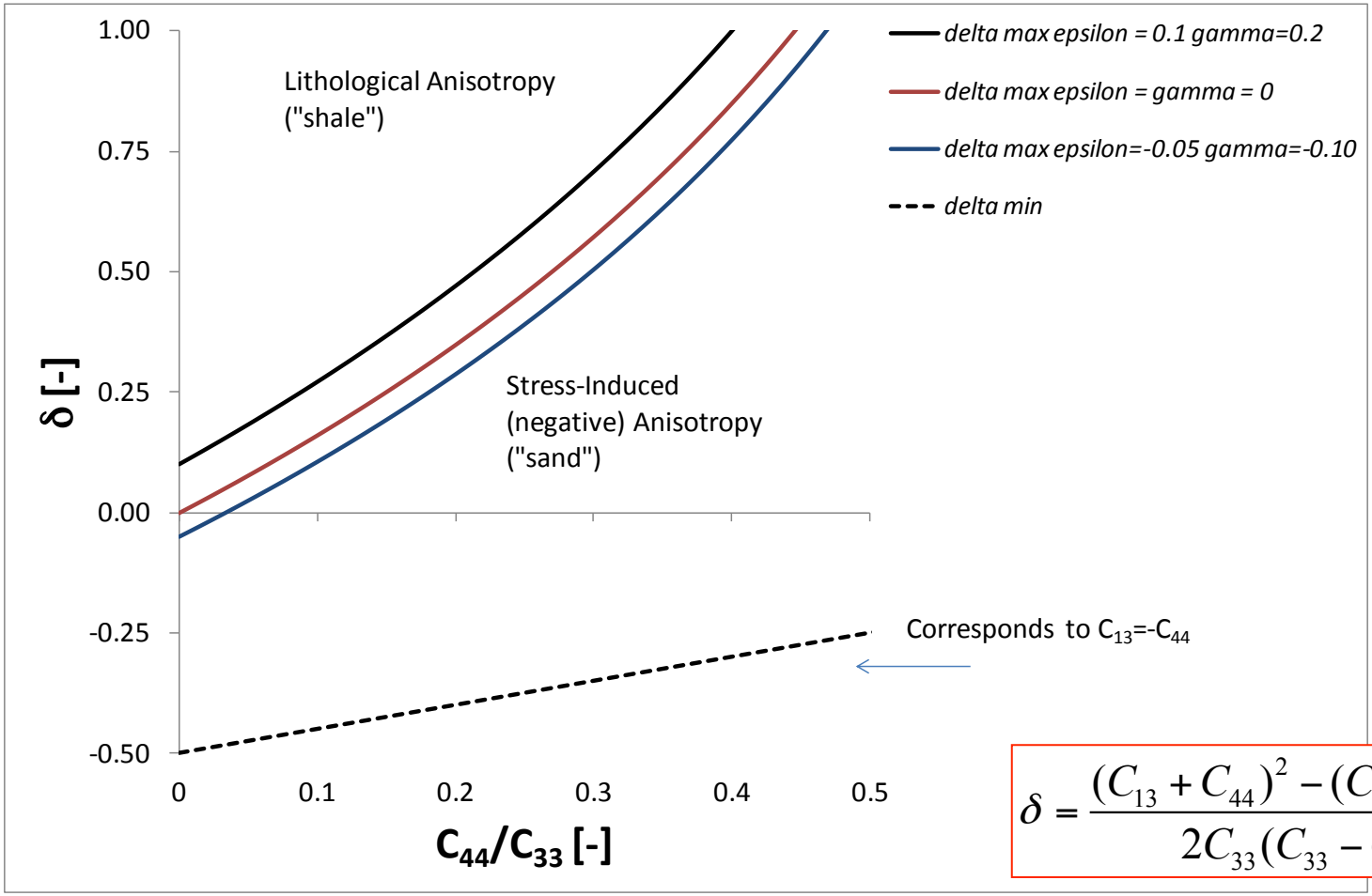

$$\delta = \frac{(C_{13} + C_{44})^2 - (C_{33} - C_{44})^2}{2C_{33}(C_{33} - C_{44})}$$

Static Mechanical Anisotropies; Mancos Shale

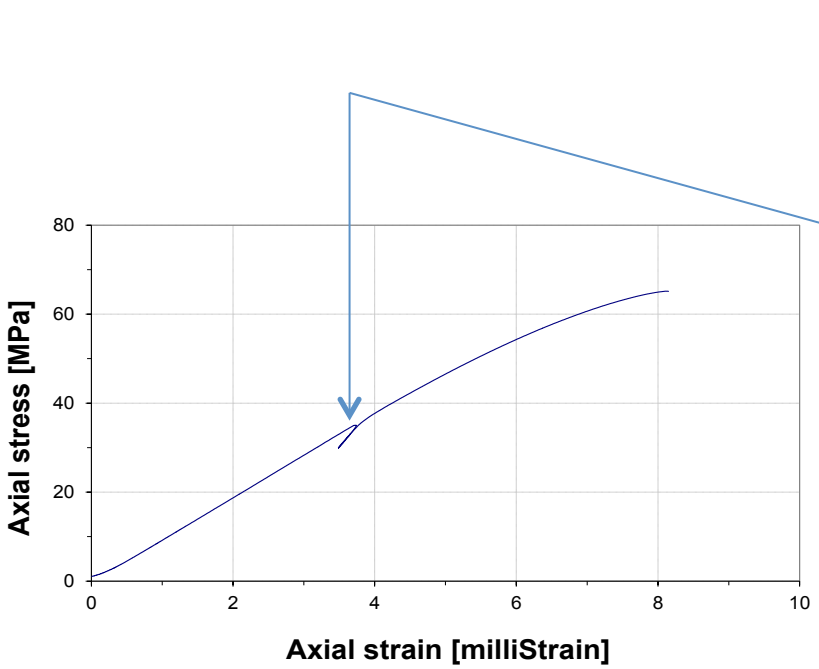

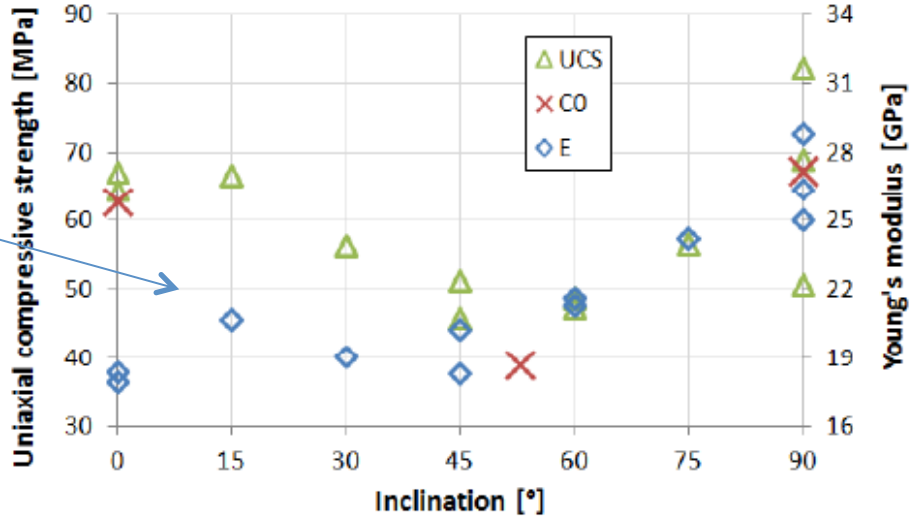

Nes & Fjær, ARMA 2013

- Idea of "patchy" plane of weakness may explain observed strength anisotropy

8% porosity, 24% clay, unsaturated

Mancos Shale: Ultrasonic P-Wave Anisotropy

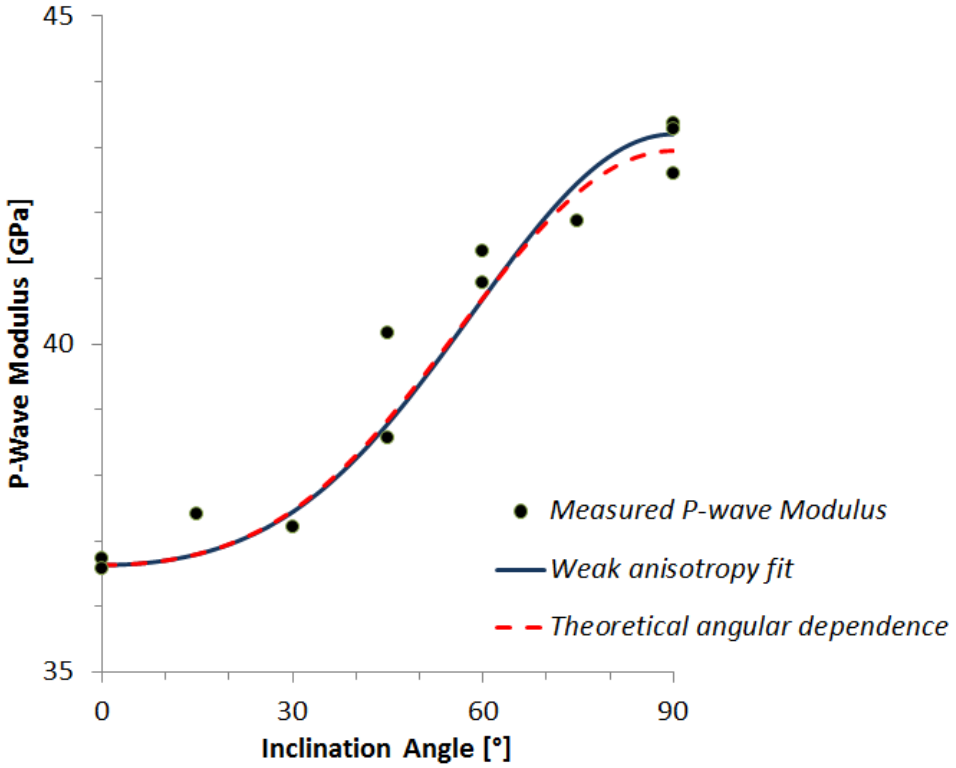

Thomsen parameters used in fit:
$\varepsilon = 0.086$
$\gamma = 0.152$
$\delta = 0.03$

- Velocity measured under unconfined conditions using several core plugs

Mancos Shale: E-Modulus Anisotropy

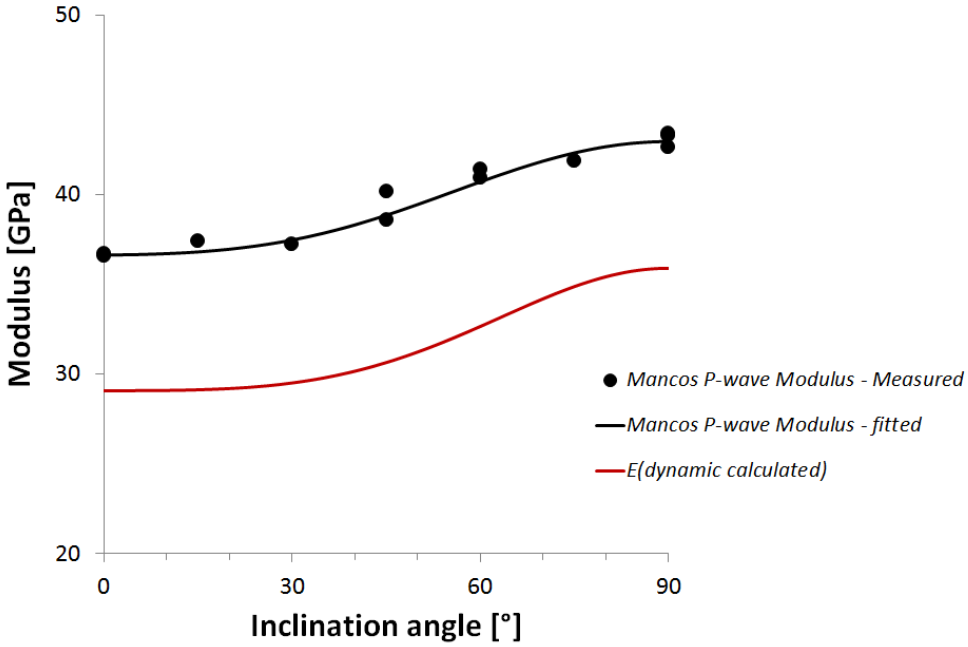

- E-modulus predicted from ultrasonic velocities, accounting for observed P- and S-wave velocity anisotropy

$$\frac{1}{E(\theta)} = \frac{1}{E_{\perp}}\cos^4\theta + \frac{1}{E_{\mathrm{P}}}\sin^4\theta + \frac{1}{B}\sin^2\theta\cos^2\theta$$

Same parameters used in fit for P-wave modulus and E

$$E_{\perp} = \frac{\left[C_{33}(C_{11}-C_{66})-C_{13}^2\right]}{(C_{11}-C_{66})} \approx \frac{C_{44}(3C_{33}-4C_{44})}{(C_{33}-C_{44})}\left[f_{\perp}(C_{IJ},\varepsilon,\gamma,\delta)\right]$$

$$E_{\mathrm{P}} = \frac{4C_{66}[C_{33}(C_{11}-C_{66})-C_{13}^2]}{(C_{11}C_{33}-C_{13}^2)} \approx \frac{C_{44}(3C_{33}-4C_{44})}{(C_{33}-C_{44})}\left[f_{\mathrm{P}}(C_{IJ},\varepsilon,\gamma,\delta)\right]$$

$$B = etc\ldots$$

Mancos Shale: E-Modulus Anisotropy

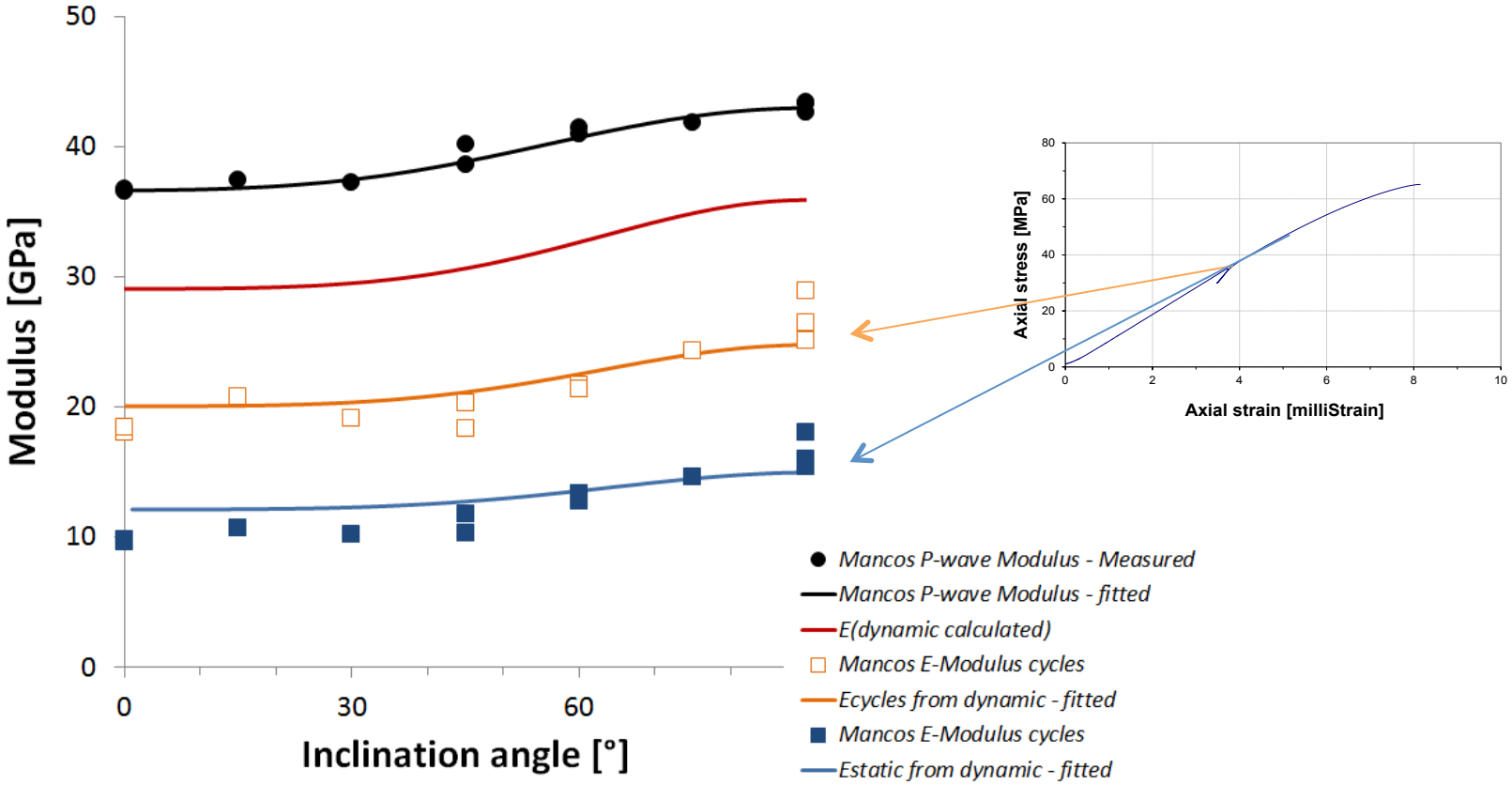

Same parameters used in fit for P-wave modulus and E

- E-modulus predicted from ultrasonic velocities, accounting for observed P- and S-wave velocity anisotropy, and reduced by a factor 1.45 to fit the measured E in cycles, and 2.5 to fit the E measured in 1st time loading

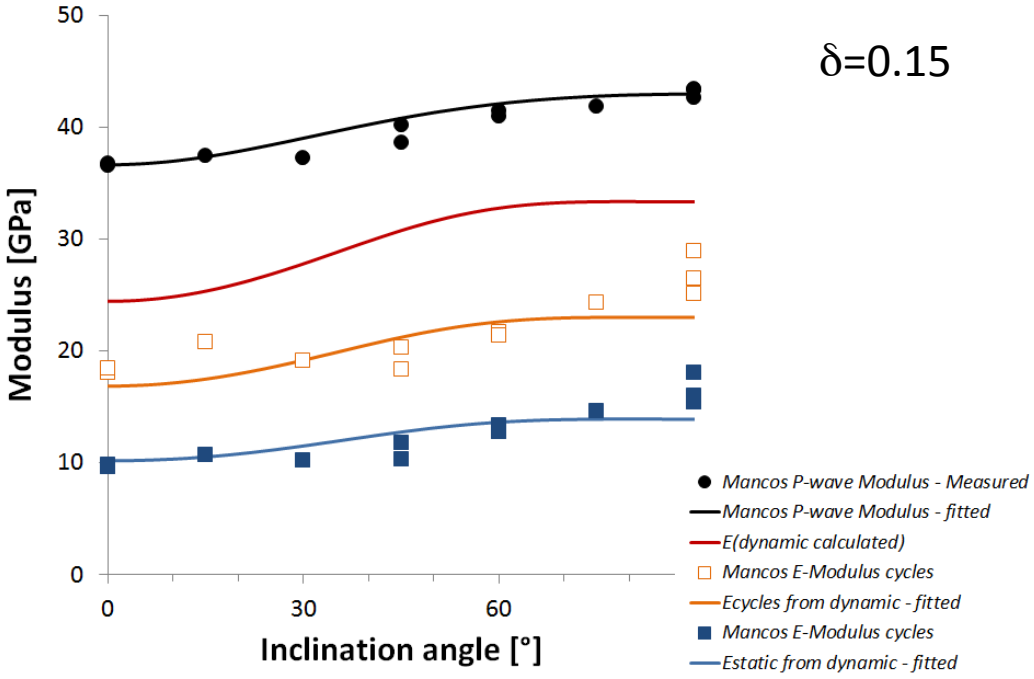

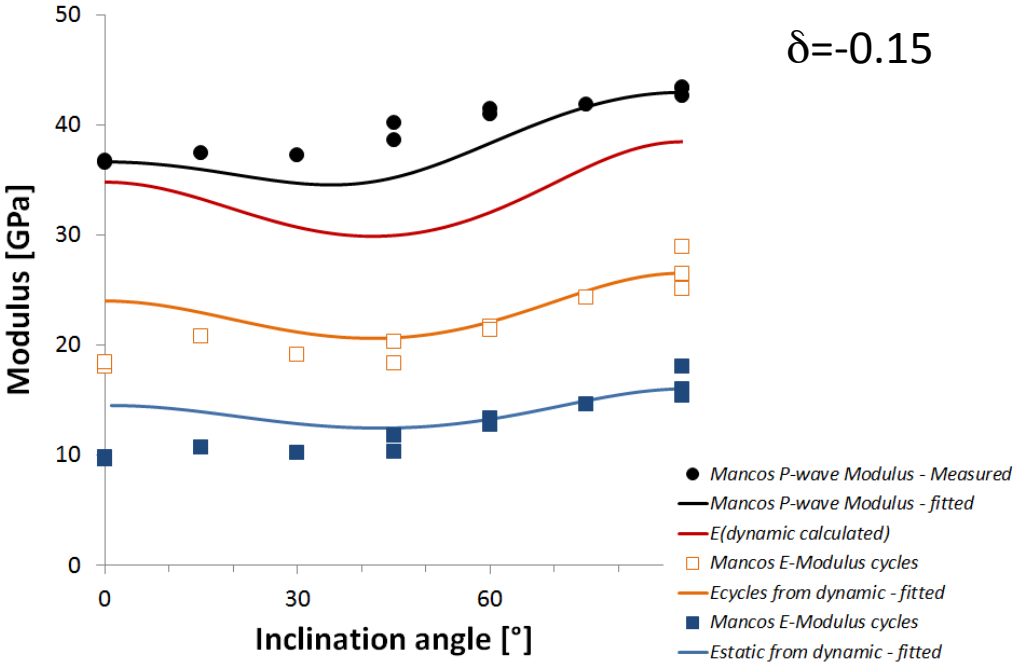

- Sensitivity of angular dependence to C13 (δ); Mancos Shale

Pierre Shale

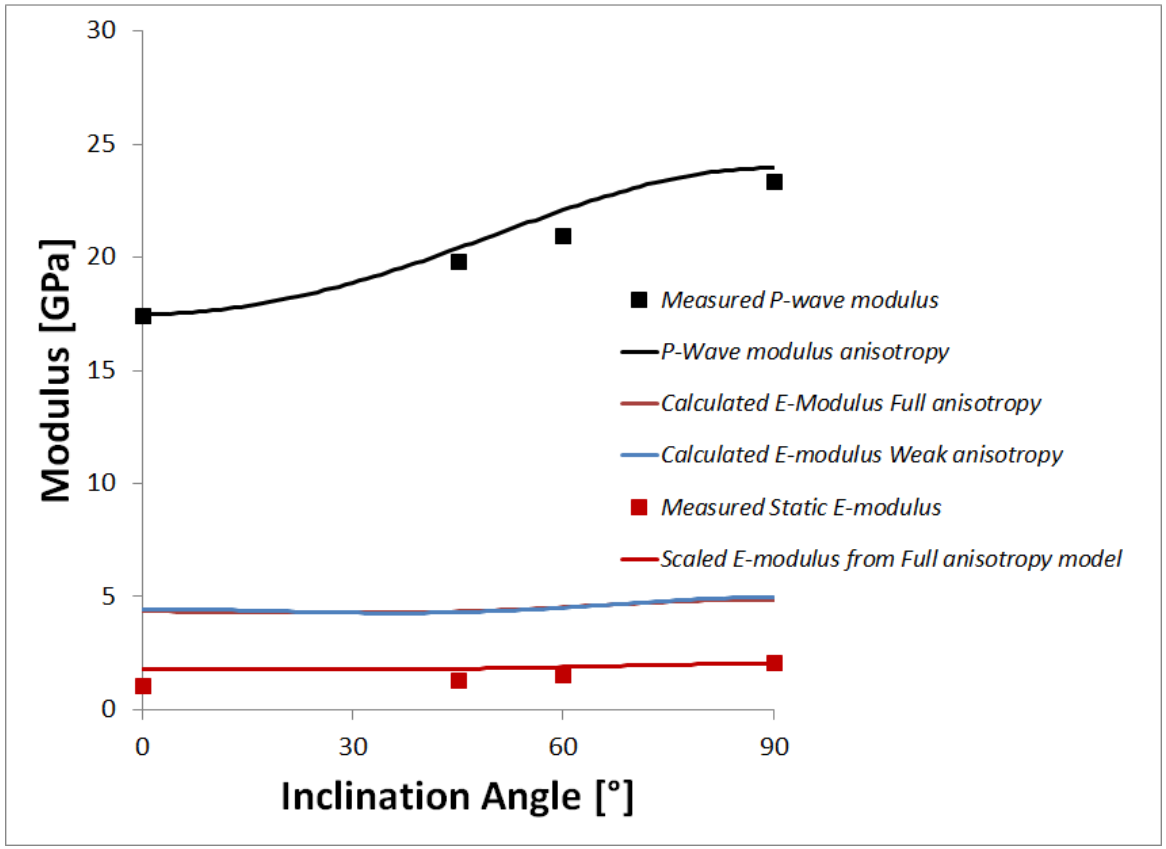

Thomsen parameters used in fit:
$\varepsilon = 0.17$
$\gamma = 0.02$
$\delta = 0.15$

Dynamic / Static scaling factor: 2.4

- 25 MPa confining pressure, 10 MPa pore pressure

19-26% porosity, 40-60% clay, brine saturated

Field Shale

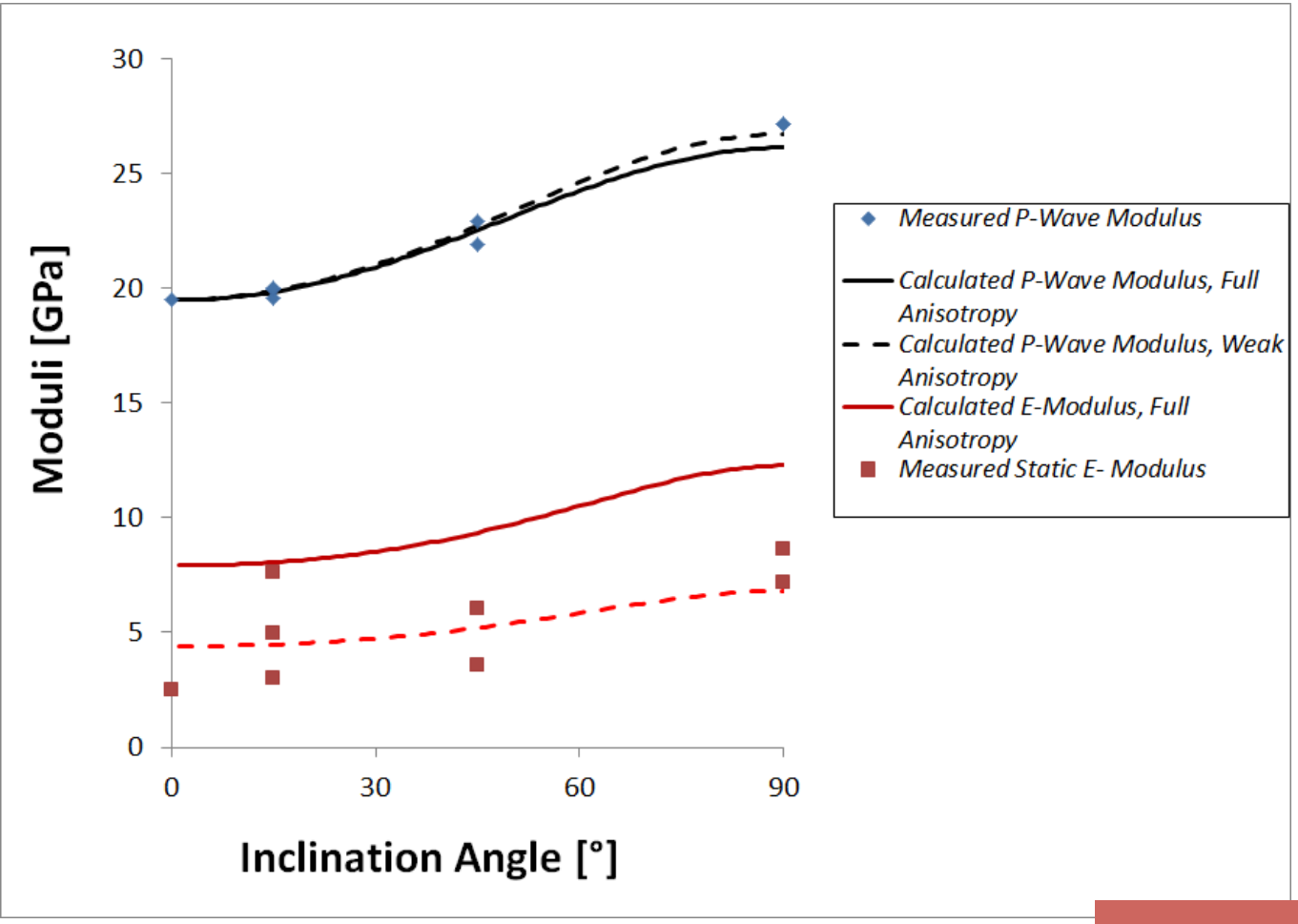

Thomsen parameters used in fit:

$\varepsilon = 0.171$

$\gamma = 0.235$

$\delta = 0.150$

Dynamic / Static scaling factor: 1.8

These shales have

15% porosity, 50-60% clay, brine-saturated

Conversion between Static & Dynamic Anisotropy

- Moduli are very different, but the angular dependence appears within measurement uncertainty to be described by the dynamic anisotropy parameters

Why are Static ≠ Dynamic Moduli?

Fluid contribution

Static
drained (normally)

Dynamic
undrained (always)

$$K_{fr} \quad \leftrightarrow \quad K_{fr} + K_f \frac{\alpha^2}{\phi + \frac{K_f}{K_s}(\alpha - \phi)}$$

Negligible for gas saturation

Dispersion

Ultrasonic: f ~ 1 MHz

Sonic: f ~ 10 kHz

Static: f ~ 1 Hz

Plasticity

Static moduli are measured at finite strains and include elastic + plastic deformation; Dynamic moduli are measured at infinitesimal strain and are hence purely elastic.

+ Scale effects, Anisotropy, a.o.

Dispersion in Mancos Shale

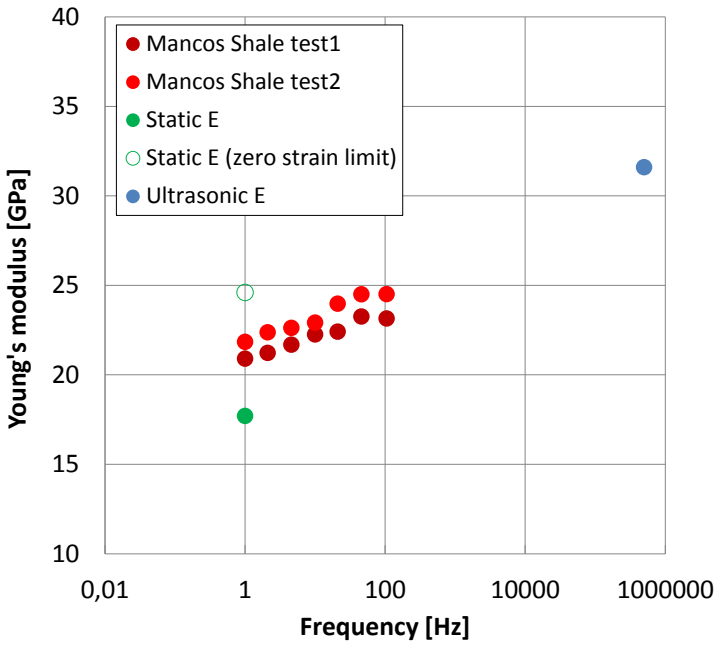

Experiment performed @ ambient conditions

- Ultrasonic : Seismic Modulus ~ 1.5
- A part of static vs dynamic discrepancy in Mancos Shale stems from dispersion
- Possible mechanisms: Viscous shear relaxation / Bound water effect or Patchy saturation?

Mancos Shale: E-Modulus Anisotropy

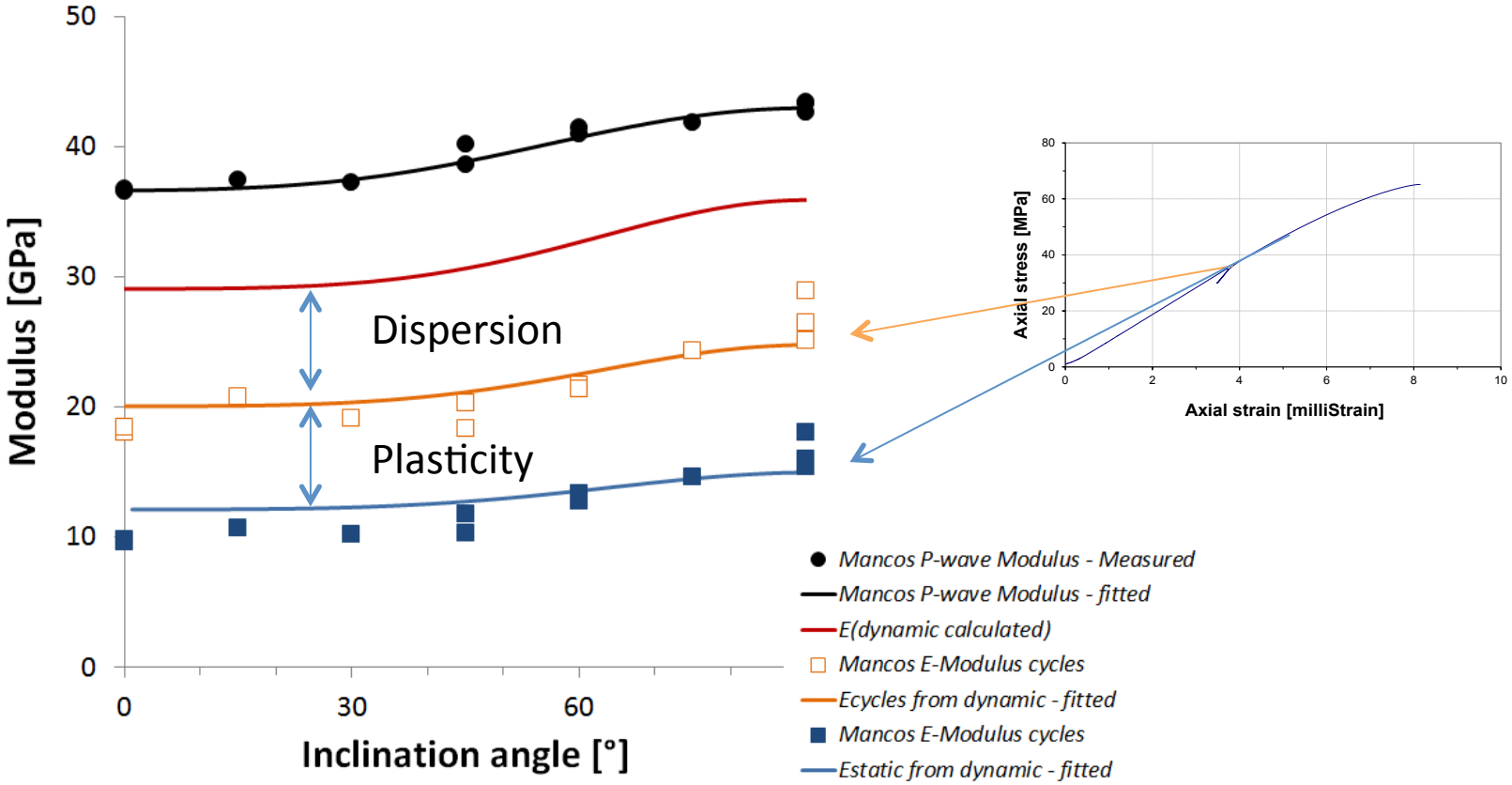

Same parameters used in fit for P-wave modulus and E

- E-modulus predicted from ultrasonic velocities, accounting for observed P- and S-wave velocity anisotropy, and reduced by a factor 1.45 to fit the measured E in cycles, and 2.5 to fit the E measured in 1st time loading

Measured δ vs. theoretical bounds

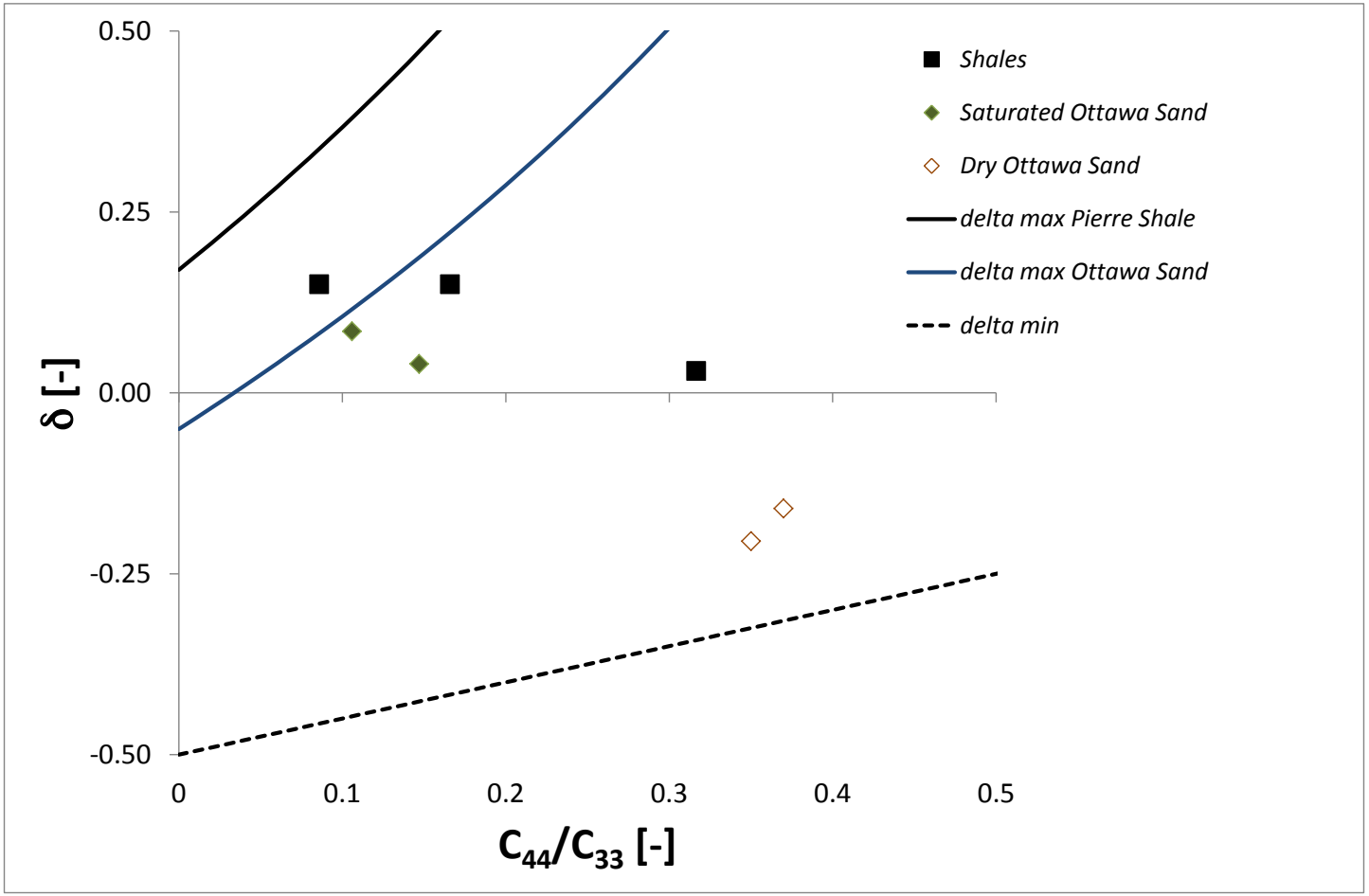

Sand data from Ph.D. work of Bhuiyan (2014 + N)*

*N<1

Conclusions

- Dynamic E-moduli by far exceed static moduli in the shales studied, because of:
  - Non-elastic deformation
  - Dispersion
- Reasonable angular dependence of static E-modulus may be deduced from wave velocity anisotropy, using a fixed scaling parameter + dynamic anisotropy parameters
- C_{13} (or δ) is crucial for angular dependence
  - Bounds on C_{13} may be used to guide interpretation
  - For soft & saturated shale (+ sand) the maximum permitted value of δ may be <0

Acknowledgements to SIP on Gas Shale @ SINTEF Petroleum Research + Statoil for funding of rock mechanics tests + The Norwegian Research Council and industry for support to ROSE @ NTNU and Shale Rock Physics @ SINTEF

Plasticity in Mancos Shale

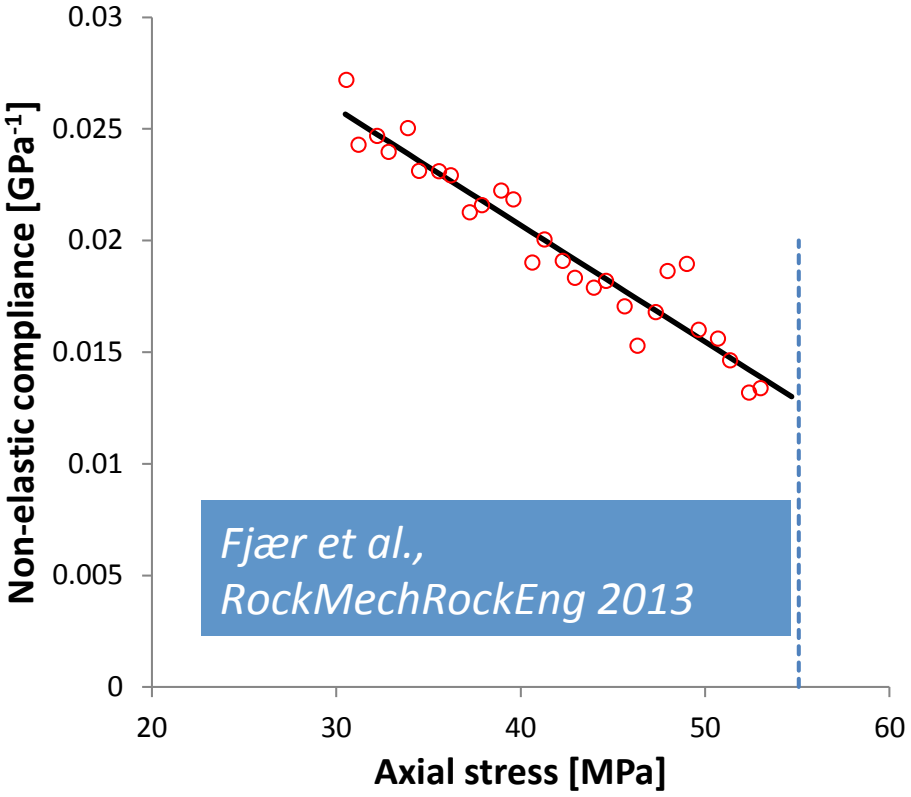

$$\frac{1}{H_{non-el}} = \frac{1}{H_{stat}} - \frac{1}{(\rho v_P^2)}$$

Here: Estimated dispersion 20 %

The non-elastic compliance should disappear near turning points of the stress path, where the material behaves elastically

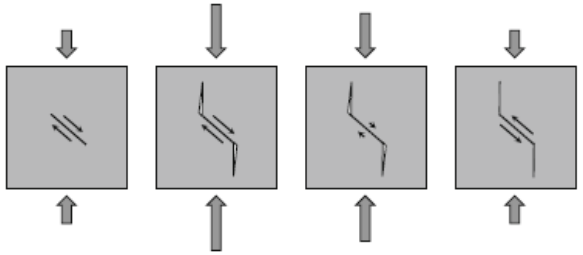

In a uniaxial strain experiment, static modulus corresponds to P-wave modulus

Non-zero non-elastic compliance when extrapolating to the turning point represents dispersion between quasi-static and ultrasonic frequency